Journal of Thermal Analysis, Vol. 29 (1984) 733–743

CRYSTALLIZATION OF GLASSES IN THE SYSTEM SiO_2–Li_2O–TiO_2–Al_2O_3, INVESTIGATED IN SITU AT HIGH TEMPERATURE BY XRD AND DTA METHODS

*A. Benedetti, G. Fagherazzi, S. Meriani** and *G. Sorarù***

DIPARTIMENTO DI SPETTROSCOPIA, ELETTROCHIMICA E CHIMICA FISICA, UNIVERSITÀ DI VENEZIA, CALLE LARGA S. MARTA D. D. 2137, 30123 VENEZIA, * ISTITUTO DI CHIMICA APPLICATA DELL'UNIVERSITÀ DI TRIESTE, VIA VALERIO 2, 34127 TRIESTE, ** ISTITUTO DI CHIMICA INDUSTRIALE DELL'UNIVERSITÀ DI PADOVA, VIA MARZOLO 9, 35200 PADOVA, ITALY

The processes of crystallization of fibres (diameter 10–15 μm) and coarse powders (grain size 500–1000 μm) with four compositions in the system SiO_2–Li_2O–TiO_2–Al_2O_3 were studied by conventional and in situ high-temperature XRD, DTA, SEM and optical microscopy. Activation energies of crystallization and morphological indices were deduced from the kinetic curves obtained by recording the high-temperature XRD peak intensity as a function of time. The glass-ceramic fibres drawn from compositions which exhibit glass-in-glass phase separation show prevailing not-oriented bulk crystallization, whereas prevailing surface crystallization was found for single-phase glass fibres. Homogeneously-dispersed crystallization was obtained on heating fibres of these compositions. The partially co-crystallized glass fibres of eutectic composition between Li-metasilicate and β-spodumene gave rise to a very fine and homogeneously-dispersed sub-microstructure.

The aim of the present investigation was the study of the processes of crystallization of glasses in the SiO_2–Li_2O–TiO_2–Al_2O_3 system, either as fibres or as coarse powders. The materials were characterized by means of differential thermal analysis (DTA), electron (SEM) and optical microscopy, and X-ray diffraction (XRD). This latter analysis was performed either at room temperature on quenched samples, or directly in situ at high temperature during the crystal growth process. For this purpose, a high-temperature attachment (1100° max.), built for vertical diffractometers [1, 2] was successfully employed.

This investigation is part of a wider research programme [3–7] concerning partially-crystallized glassy fibres with a controlled microstructure. A knowledge of the formation mechanisms of these microstructures may lead to the development of new reinforced materials containing glassy fibres.

Four chemical compositions, denoted G1, G3, G6 and G7, were chosen (see Figs 1 and 2 and Table 1). The first three glasses are based on the Li–Ti-silicate system,

with a small and constant amount (mol %) of Al_2O_3. The fourth is the eutectic composition between Li-metasilicate and beta-spodumene (Li_2SiO_3–$LiAlSi_2O_6$) with an addition of titania (TiO_2).

The first three compositions were selected in order to determine if the presence of a glass-in-glass phase separation could give a higher homogeneity of dispersion among the involved phases. Instead, the composition G7 was chosen with the purpose of obtaining eutectic co-crystallization, which should give rise to a microstructure of very small and homogeneously-dispersed crystallites. This latter composition was also used by Barry et al. [8] to obtain glass-ceramic bodies with good mechanical properties. On the other hand, the first three glasses, apart from the alumina content, have previously been investigated by Fields et al. [9] with the aim of strengthening the initial glassy phase by phase separation.

Experimental

The composition in mol % of each examined glass is reported in Table 1 (weight % within parentheses) and graphically indicated in the ternary diagrams of Figs 1 and 2, drawn from the literature [10, 11]. The method of production of the fibres, which have a diameter of 10–15 μm, was described elsewhere [3–5]. The thermal evolution of the glassy systems was studied with a DTA apparatus (Netzsch) and by XRD, using a vertical diffractometer (Philips) equipped with the above-mentioned high-temperature attachment, a graphite focussing monochromator, a high-power X-ray tube (Cu K-alpha radiation) and a scintillation counter.

Table 1 Chemical composition in mol% of the glassy systems (weight % within parentheses)

Oxide	Glassy systems			
	G1	G3	G6	G7
SiO_2	70 (77.8)	70 (75.0)	70 (72.4)	53.7 (58.9)
Li_2O	25 (13.7)	21 (11.1)	17 (8.7)	32.1 (17.5)
TiO_2	2 (2.9)	6 (8.5)	10 (13.6)	7.0 (10.2)
Al_2O_3	3 (5.6)	3 (5.4)	3 (5.2)	7.2 (13.4)

The microstructures of the partially-crystallized materials were examined by SEM (Cambridge) and optical microscopy. DTA experiments were carried out under the following conditions: heating rate 10 deg./min; sensitivity 0.1 mV for full-scale expansion; 200 mg of sample *vs.* 200 mg of alumina in specimen holders of sintered alumina. The XRD measurements on the quenched samples were performed with a goniometer scanning rate of 0.25 deg./min and a time constant RC = 4 sec, whereas the XRD high-temperature conditions were 1 deg./min and 4 sec, respectively.

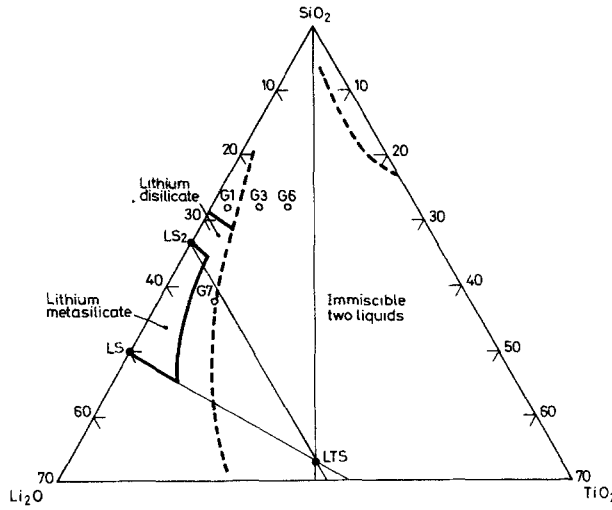

Fig. 1 Phase diagram Li_2O–SiO_2–TiO_2, % mol (Ref. [10], [11]). LTS = Li_2TiSiO_5

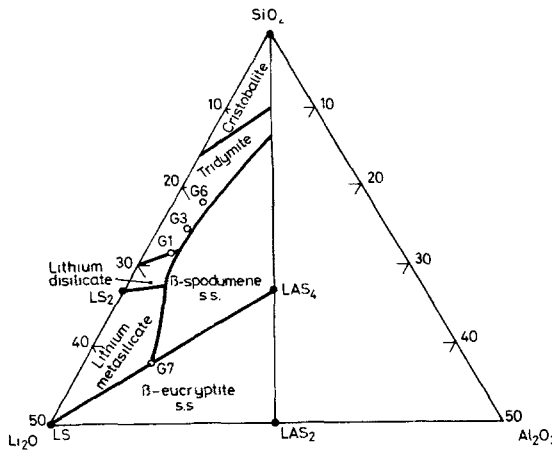

Fig. 2 Phase diagram Li_2O–SiO_2–Al_2O_3, % mol (Ref. [10], [11]). LS = Limetasilicate, LAS_4 = = β-spodumene, LAS_2 = β-eucryptite

Results and discussion

DTA and room-temperature XRD analysis

Figure 3 shows the DTA curves of G1, G3, G6 and G7 fibres and of G1 and G7 coarse powders ground down to 500–1000 μm. The first exothermic peaks for the coarse powder samples (G1 and G7) are found at higher temperatures than the corresponding peaks for the fibres. This behaviour may be due to a contribution of surface

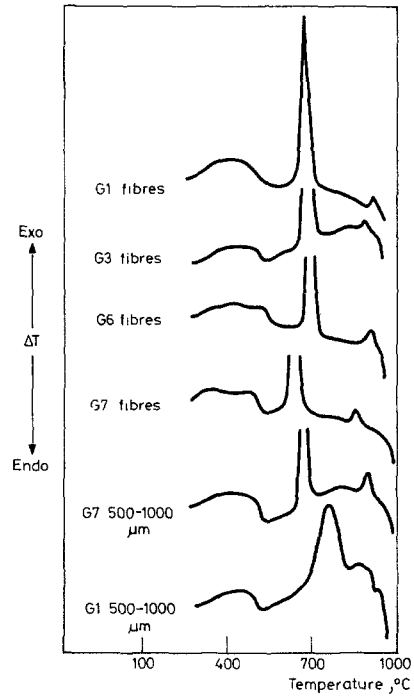

Fig. 3 DTA traces for G1, G3, G6 and G7 compositions either as fibres or as coarse powders

crystallization in the fibrous materials. The DTA traces are all similar. An endothermic effect, due to the glass transition, is present in the temperature interval 470–530°. The maximum of the first strong exothermic peak is situated between 640 and 760°, while a much smaller effect is observed between 860 and 930°. The first exothermic peak is due to a simultaneous crystallization of two phases. They are beta-quartz and Li-disilicate for systems G1, G3 and G6, whereas for G7 beta-eucryptite ($LiAlSiO_4$) and Li-metasilicate (Li_2SiO_3) were found after the first crystallization. We believe that the β-quartz phase found in G1, G3 and G6 is a solid solution containing a small amount of Al^{3+} and Li^+ ions, with unit cell parameters $a_0 = 5.020 \pm 0.005$ Å and $c_0 = 5.425 \pm 0.005$ Å, which are very close to those reported for pure beta-quartz [12]. These substitutional Al^{3+} and interstitial Li^+ ions are likely to favour the high-quartz structure rather than the low-quartz alpha form. To assess the role of Al^{3+}, we prepared a glass which had the same relative composition as G6 in terms of Si, Li and Ti, but did not contain any aluminum. In this system, alpha-quartz and not beta-quartz was obtained on crystallization.

The hexagonal unit cell constants found for beta-eucryptite in G7 are meaningfully shorter ($a_0 = 5.203 \pm 0.003$, $c_0 = 10.86 \pm 0.01$ Å) than those of the stoichiometric phase [13] ($a_0 = 5.27$, $c_0 = 11.25$ Å). The solid solution, indicated as beta-eucryptite s.s., shows a very strong analogy with the structure of beta-quartz, since it originates

from the latter by progressive enrichment of Li^+ and Al^{3+}, with a final superlattice ordering along the *c*-axis [14].

An interpretation of the small second exothermic DTA peak was given for systems G1, G3 and G6 in a previous work [7]. For system G7 it is certainly due to the beta-eucryptite s.s. transition into beta-spodumene, which was also found to take place in other systems [2]. Further investigations of the formation of the crystalline phases which develop after the first DTA peak at about 930° will be reported elsewhere [15]. It is worth mentioning that, with the exception of beta-spodumene, all the phases so far identified contain titanium.

It is also worth noting that all the unit cell parameter refinements were carried out with data taken on samples quenched after thermal treatment for 2 hours at a temperature close to the maximum of the first exothermic DTA peak.

High-temperature in situ XRD analysis

The XRD diagrams directly obtained in situ at high temperature (Fig. 4) clearly show that the two phases β-quartz s.s. and Li-disilicate simultaneously crystallize in systems G1, G3 and G6, while the two phases beta-eucryptite s.s. and Li-metasilicate simultaneously crystallize in system G7. As an example of the experimental data, the crystallization isotherm relating to G6 fibres, recorded at 620°, is reported in Fig. 5. In these curves the XRD peak heights are plotted *vs.* time. Two pairs of reflections (101—100) for beta-quartz s.s. and (111—130) for Li-disilicate, are reported. Good agreement for the trends in each pair of curves was obtained by linearizing them with the Avrami equation [16]. The strongest reflections for beta-quartz (101) and Li-disilicate (111) were measured, in order to carry out a kinetic study of the multiphase transformation involved in the first exothermic DTA peak. Figure 6 shows the

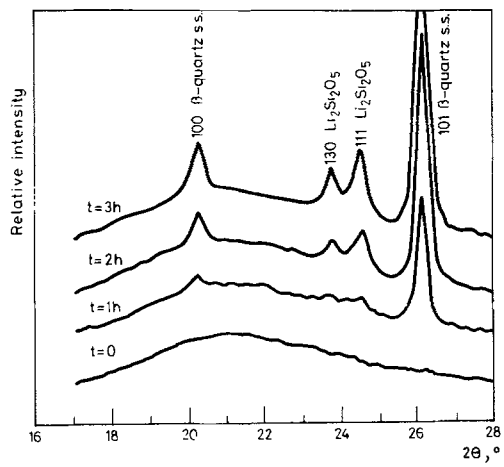

Fig. 4 XRD high temperature patterns of G6 at 620 °C after various heating time

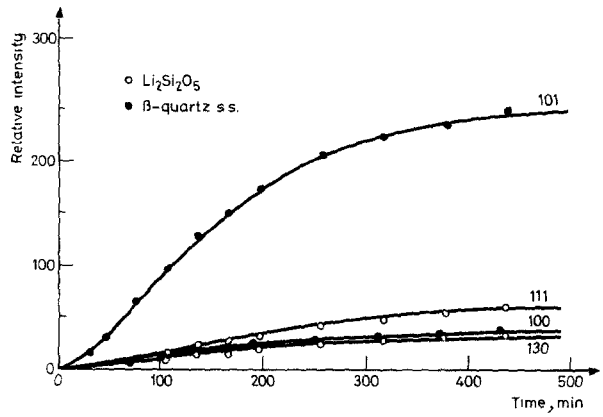

Fig. 5 (101–100) peak height intensity of beta-quartz and (111–130) peak height intensity of $Li_2Si_2O_5$ *vs.* time, for fibres of composition G6 isothermally heated at 620 °C. The measurements have been performed *in situ* with a high temperature device for X-ray vertical diffractometers

crystallization kinetic curves, obtained isothermally at different temperatures for G7 fibres, employing the (102) reflection of beta-eucryptite and the (111–021) reflections of Li-metasilicate.

It is worth noting that the validity of these kinetic curves, which obviously give relative values of crystallinity, was checked in a previous work [18] by using the absolute method of Ruland [19] for determination of the crystallinity of organic polymers, as modified by Vonk and Fagherazzi [20] for glass-ceramic materials.

The interpretation of all the kinetic curves similar to those reported in Fig. 6 was performed in the framework of the Avrami theory, as recently revised by Christian [17]. Table 2 reports the values, E_{cryst}, of the activation energy for crystallization, as well as the morphological index, n, or reaction order in this case, obtained by applying the classical Avrami equation. The n indices reported in Table 2 might be influenced by diffusion phenomena of the ions making up the crystalline structure, at a relatively long distance from the crystal-glass interface. Nevertheless, in the present case this influence must be considered negligible since the crystallization process involves phases of composition fairly close to that of the initial glass. The n values reported in Table 2, which are all between 1 and 2, therefore suggest that the contribution of the surface crystallization is meaningful, especially for G1 and G7 fibres which exhibit lower n values. The formation of non-equiaxial crystallites, like the acicular ones of Li-disilicate, also contribute to the lowering of the n values.

It is worth pointing out that some measurements of E_{cryst} and n, carried out on not pre-treated samples, gave values similar to those reported in Table 2. For example, not pre-treated G1 fibres gave values of 263 kJ/mol and 372 kJ/mol for the crystallization energies of Li-disilicate and beta-quartz, respectively.

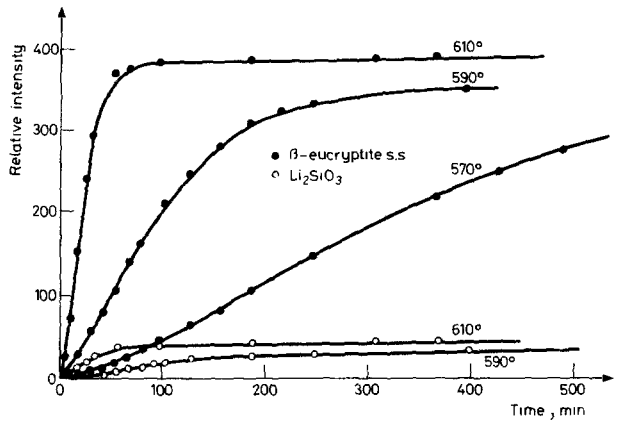

Fig. 6 Peak height intensity vs. time of (102) beta-eucryptite and (111–021) Li_2SiO_3 reflections for fibres of composition G7 isothermally, heated at various temperatures

Table 2 Activation energy of crystallization, $E_{cryst.}$, and morphological indices, n, deduced from the XRD kinetic curves obtained at high temperature. All the samples were thermically pre-treated

Sample	$E_{cryst.}$, kJ/mol		n	
	β-quartz s.s.	$Li_2Si_2O_5$	β-quartz s.s.	$Li_2Si_2O_5$
G1 (Fibres)	493	380	1.7	1.4
G3 (Fibres)	447	468	1.8	1.9
G6 (Fibres)	531	522	1.5	1.6
	β-eucryptite s.s.	Li_2SiO_3	β-eucryptite s.s.	Li_2SiO_3
G7 (Fibres)	472	309	1.4	1.6
G7 (500–1000 μm)	543	685	1.9	1.9

Textural and sub-microstructural features

Qualitative investigations on the preferred crystalline orientation were performed with a photographic cylindrical camera on the partially-crystallized fibres, placed as a bundle within a capillary X-ray glass [15]. The main results of this study showed that, for composition G1, the crystallites of Li-disilicate preferentially grew from the surface, down into the fibre core, with their c_0 axis of the orthorhombic unit cell perpendicular to the external surface, whereas beta-quartz s.s. did not show any orientation.

G7 fibres also display a very complex preferential crystalline orientation, either for Li-metasilicate or for beta-eucryptite s.s. In contrast, for compositions G3 and G6, no evidence of preferred crystalline orientation could be detected. All these results agree with the presence of surface crystallization on the G1 and G7 fibres.

It is worth noting that the XRD peaks of beta-eucryptite s.s. and Li-metasilicate appear fairly broadened in G7 fibres heated in the range 570–610°. Application of an appropriate Scherrer formula [21] led to a value of 150±50 Å for the average crystallite size of both phases. This fine sub-microstructure was indirectly confirmed by SEM observations of fracture surfaces (Fig. 7), which had a texture which could not be resolved by our apparatus. Moreover, in this figure, no evidence of strong sintering effects between fibres is seen.

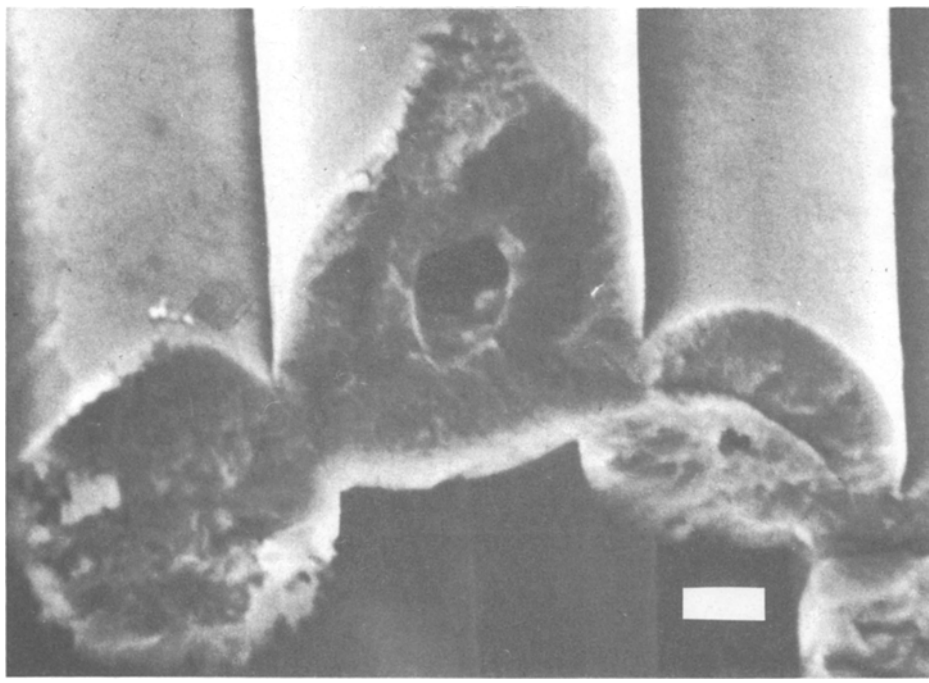

Fig. 7 SEM image of fibres G7 heat treated at 580 °C for 1 hour and etched 15 sec with 2% HF solution to evidentiate microstructure. The bar corresponds to 3 μm

Kinetic study by optical methods

The surface layer growth was followed by means of optical microscopy on bulk samples with compositions G1 and G3 treated at three different temperatures within the range 630–690°. In this way, diagrams similar to that in Fig. 8 were obtained. They demonstrate that the crystalline layer growth, v, is linear with time and allows calculation of the growth rate. The activation energy is obtained as the slope of the $\ln(v)$ *vs.* $1/T$ diagram, as reported in Fig. 9 for the composition G1. The activation energies for G1 and G3 are 263 kJ/mol and 305 kJ/mol, respectively. In the case of G6, this method could not be applied effectively because the crystallization front

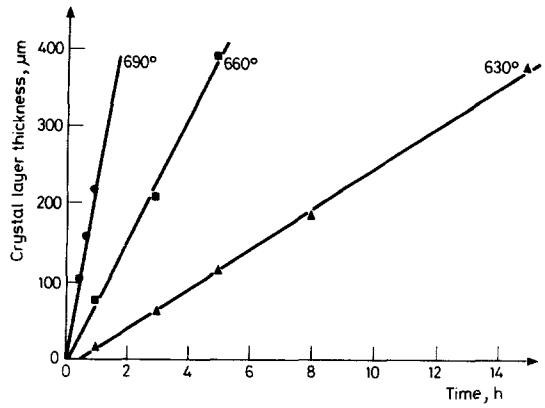

Fig. 8 Thickness of external crystalline layer *vs.* time in G1 heat treated composition glass fragments

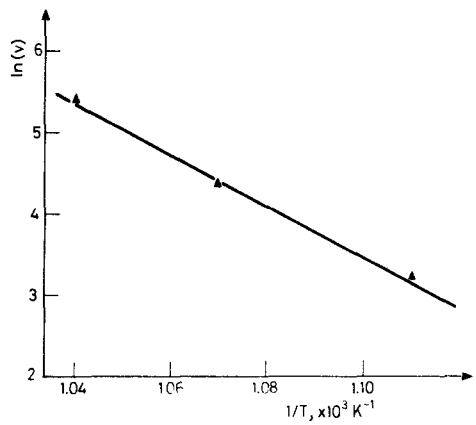

Fig. 9 Arrhenius plot for the crystallization kinetics of bulk glass G1

was constrained by the diffuse bulk crystallization. For compositions G1 and G3, the values obtained for the crystallization energy are in fairly good agreement with those obtained with the XRD method.

Conclusions

The thermal evolution of glass-ceramic fibres, treated according to heating schedules derived from DTA measurements, was studied by either in situ high-temperature or conventional XRD, SEM and optical microscopy. All the collected evidence on activation energies, reaction orders, preferred crystalline orientation and sub-microstructural features allow the following general statements to be made:

a) Glass-ceramic fibres drawn from compositions which exhibit glass-in-glass phase separation (G3 and G6) undergo prevailing not-oriented bulk crystallization, whereas prevailing surface crystallization was found for single-phase glass fibres (G1). Homogeneously-dispersed crystallization was obtained on heating fibres of the composition G6.

b) The partially co-crystallized glass fibres of eutectic composition G7 gave a very fine and homogeneously-dispersed sub-microstructure, the size of which was beyond the resolution limits of the available SEM techniques, but was estimated to be in the range 150±50 Å by means of X-ray line-broadening analysis. Some surface contribution to the overall crystallization process in G7 fibres is also present.

The purpose of this investigation, which was to prove that glass-in-glass phase separation and eutectic compositions favoured homogeneous bulk crystallization, was satisfactorily achieved and, within the aim of this research programme, fibres will be tested for their mechanical properties in a forthcoming investigation.

* * *

This work was supported by the Italian C. N. R., "Progetto Finalizzato Chimica Fine e Secondaria – Sottoprogetto Metodologie".

We are indebted to Dr. B. Locardi of Stazione Sperimentale del Vetro, Murano (Venice) for furnishing the initial glasses and fibres.

We are also indebted to the "G. Giacomello" Institute (C. N. R., Rome) for furnishing the computer programme for the unit cell parameter refinement. Assistance by M. Pistolato and F. Venuda in the experimental work is gratefully acknowledged.

References

1 G. Spinolo, V. Massarotti and G. Campari, J. Phys. E. Sci. Instrum., 12 (1979) 1059.
2 A. Benedetti, G. Fagherazzi and S. Meriani, J. Mater. Sci., 18 (1983) 2510.
3 S. Meriani, B. Locardi, F. Barbon, G. Scarinci and G. Sorarù, Science of Ceramics, Col. 11; R. Carlsson and S. Karlsson Ed., Swedish Ceramic Society, Gotheborg, Sweden, 1981, p. 321.
4 A. Benedetti, G. Cocco, G. Fagherazzi, B. Locardi and S. Meriani, J. Mater. Sci., 18 (1983) 1039.
5 A. Benedetti, G. Cocco, G. Fagherazzi, S. Meriani and G. Scarinci, J. Mater. Sci., 18 (1983) 1049.
6 S. Meriani, G. Fagherazzi, B. Locardi and G. Sorarù, Thermal Analysis, Vol. 1, Proceedings of the 7th Inter. Conf. in Thermal Analysis, B. Miller Ed., John Wiley, New York, 1982, p. 660.
7 S. Meriani, A. Benedetti, D. R. Festa, B. Locardi, G. Scarinci and G, Sorarù, Science of Ceramics, P. Vincenzini Ed., Ceramurgica spl. Faenza, 1983, p. 419.
8 T. I. Barry, D. Clinton, L. A. Lay, R. A. Mercer and R. P. Miller, J. Mater. Sci., 4 (1969) 596.
9 J. M. Fields Jr., W. D. Leahy and J. Brown Jesse Jr., Paper presented at the 72nd Annual Amer. Ceram. Soc. Convention, Philadelphia, Pennsylvania, 1970.
10 Phase Diagrams for Ceramists, fig. 449, E. Levin et al., Am. Ceram. Soc., 1964, p. 166.
11 Phase Diagrams for Ceramists, fig. 474, E. Levin et al., Am. Ceram. Soc., 1964, p. 172.
12 W. A. Basset and D. M. Lapham, The Am. Mineralogist, 42 (1957) 548.

13 H. G. F. Winkler, Acta Cryst., 1 (1948) 27.
14 G. H. Beall, B. R. Karstetter and H. L. Rittler, J. Am. Ceram. Soc., 50 (1967) 181.
15 G. Sorarù, G. Fagherazzi, M. Bottarelli and A. Benedetti, J. Mater. Sci., accepted for publication.
16 M. Avrami, J. Chem. Phys., 7 (1939) 1103. idem, ibid., 8 (1939) 212.
17 J. W. Christian, The Theory of Transformations in Metals and Alloys, Part I, Pergamon Press, Oxford, 1975, p. 525.
18 A. Benedetti, M. Bottarelli and G. Fagherazzi, J. Non-Crystal. Solids, submitted for publication.
19 W. Ruland, Acta Cryst., 14 (1961) 1180.
20 G. C. Vonk and G. Fagherazzi, J. Appl. Cryst., 16 (1983) 274.
21 J. I. Langford and A. J. C. Wilson, J. Appl. Cryst., 11 (1978) 102.

Zusammenfassung – Die Prozesse der Kristallisation von Fasern (Durchmesser 10–15 μm) und groben Pulvern (Korngröße 500–1000 μm) von SiO_2–Li_2O–TiO_2–Al_2O_3 in vier verschiedenen Zusammensetzungen wurden mittels herkömmlicher und in situ XRD, DTA, SEM und optischer Mikroskopie untersucht. Aktivierungsenergien der Kristallisation und morphologische Indices wurden aus den durch Registrierung der Intensität der Hochtemperatur-XRT-Peaks in Abhängigkeit von der Zeit erhaltenen kinetischen Kurven ermittelt. Die aus Gemischen einer die Glas-in-Glas-Phasentrennung bedingenden Zusammensetzung gezogenen Glas-Keramik-Fasern zeigen vorwiegend eine nicht-orientierte Bulk-Kristallisation, während vorherrschend Oberflächenkristallisation bei Einphasen-Glasfasern festgestellt wurde. Eine homogen verteilte Kristallisation wurde beim Erhitzen der Fasern dieser Zusammensetzungen erhalten. Bei partiell ko-kristallisierten Glasfasern einer eutektischen Mischung von Li-Metasilikat und β-Spodumen liegt eine sehr feine und homogendisperse Submikrostruktur vor.

Резюме – Процессы кристаллизации волокон (диаметр 10–15 мкм) и крупнозернистых порошков (размер зерен 500–1000 мкм) четырех составов в системе SiO_2–Li_2O–TiO_2–AL_2O_3 были изучены при обычной и высокой температурах методами диффракции рентгеновских лучей, ДТА, электронной и оптической микроскопии. Энергии активации процесса кристаллизации и морфологические индексы были определены из кинетических кривых, полученных измерением высокотемпературных рентгено-дифракционных пиков интенсивности в зависимости от времени. Стеклокерамические волокна, вытянутые из составов с фазовым разделением типв стекло-в-стекле, показали преимущественно неориентированную кристаллизацию во всем объёме, тогда как для однофазных стекловолокон-превалирующей была кристаллизация на поверхности. При нагревании стекловолокон такого состава происходила их гомогенно-диспергизованная кристаллизация.В случае стекловолокон эвтектического состава метасиликат лития – β-сподумен частично происходила их совместная кристаллизация с образованием очень мелкой и гомогенно-диспергированной субструктуры.